

Western States Section of the Combustion Institute – Fall 2015 Meeting
Hosted by Brigham Young University
October 5-6, 2015

Effects of Fuel Chemistry and Turbulence Intensity on Turbulent Consumption Speed for Large Hydrocarbon Fuels

Aaron J. Fillo¹ and David L. Blunck¹

¹*Mechanical Industrial and Manufacturing Engineering, Oregon State University, 204 Rogers Hall,
Oregon State University, Corvallis, OR 97331-6001, USA*

Large hydrocarbon fuels are used for ground and air transportation and will be for the foreseeable future. Despite their extensive use, combustion of large hydrocarbon fuels in a turbulent environment is poorly understood and difficult to predict. A key combustion property for such reaction is the turbulent flame speed, which is the velocity at which a flame front propagates through a turbulent fuel and air mixture. Such information can be quite useful as a model input parameter and for validation. The objective of this study is to measure and compare the turbulent flame speed of conventional jet fuels with other large hydrocarbon fuels. The flame is produced on a fully premixed turbulent Bunsen type burner capable of independently controlling turbulence intensity, unburned temperature, and equivalence ratio. The turbulent flame speed is measured for Reynolds number and equivalence ratio ranging between 5,000-10,000 and 0.8-1, respectively. Turbulence intensities are varied between ~10% and ~20% of the bulk flow velocity. A clear sensitivity to fuel chemistry is observed and seems to be linked to aromatic and alkane content; higher flame speeds and increased stability have been measured for fuels with longer average hydrocarbon chain lengths and high alkane content. A strong sensitivity to the turbulence intensity of the flow is discovered; the turbulent flame speed increases an average of 35% for all fuels between the minimum and maximum turbulence intensity cases.

1 Introduction

Reactions in internal combustion and gas turbine engines operate at elevated temperatures and pressures and are primarily driven by turbulent premixed, and partially premixed flames [1]. These applications primarily use large hydrocarbon liquid fuels such as gasoline, diesel, and jet fuel (because of the high energy density), and will for the foreseeable future. As such, an improved understanding of turbulent combustion and its sensitivity to fuel chemistry is necessary for improved engine development and alternative fuel research.

Numerous studies have investigated the laminar flame speed of transportation fuels [2–5] to determine fuel sensitivities, but avoid the complexities associated with turbulence. For example, Kumar et al. [4] investigated atmospheric laminar flame speeds and activation energies of iso-octane and n-heptane for both pure and N₂ diluted fuel-air mixtures. Iso-octane demonstrated a consistently lower flame speed for the full range of preheat temperatures investigated. Moreover, although n-heptane demonstrated an increased stability at the lean extinction limits, the laminar flame speeds at these limits were within <10%. These differences were attributed to differences in the mass burning fluxes of the two flames. Further analysis showed that n-heptane had a higher mass burning flux for all preheat temperatures and equivalence ratios examined. This higher relative reactivity was attributed to differences in the in C₂-C₃ chemistry between the two fuels. The reaction mechanisms for iso-octane and n-heptane are well studied in [6–11]. The results of these studies reveal significant difference in intermediate species concentrations; for example n-heptane combustion produces large quantities of ethylene, whereas the iso-octane produces propene, iso-butene, and methyl radicals. The large differences between the reaction mechanisms of these neat-surrogates suggest a strong sensitivity to fuel chemistry for real fuels.

Additional work by Kumar et al. [3] demonstrated a strong sensitivity to fuel chemistry for real large hydrocarbon fuel blends. The study investigated laminar flame speeds and extinction limits of conventional and alternative fuels including, Jet-A, S-8, and pure n-decane. Jet-A and S-8 demonstrated similar propagation characteristics, yet significant differences in extinction limits. S-8 provided a more stable flame that was less susceptible to stretch induced blow off. This stability was attributed to higher alkane content. Hui et al. [2], extended the findings of Kumar and collected laminar flame speeds measurements of four component surrogate fuels. The results suggest a sensitivity of the laminar flame speed to the aromatic and alkane content of their surrogate blends. In summary, laminar flame speeds have shown a fuel

sensitivity for large hydrocarbon fuels. What is not understood is how turbulent fluctuations, such as those in practical devices, alter the flame speed.

The turbulent flame speed is a metric for assessing the effects of turbulent fluctuations, molecular transport, and fuel chemistry on turbulent combustion [12]. Four definitions of the turbulent flame speed have been proposed in the literature [13–16]: local displacement speed, global displacement speed, local consumption speed, global consumption speed. The global consumption speed represents a temporally and spatially averaged measure of reactant consumption through the flame brush. It is defined as:

$$S_{T,GC} = \frac{\dot{m}_R}{\rho_R \bar{A}_{(c)}} \quad (1)$$

where \dot{m}_R , ρ_R , and $\bar{A}_{(c)}$ are the mass flow rate of the reactants, the density of the reactants, and the mean flame area corresponding to the contour $\langle c \rangle$, respectively [15]. The contour $\langle c \rangle$ corresponds to the progress variable, c , which represents reactant consumption relative the flame brush area. Here $\langle c \rangle = 0$ and $\langle c \rangle = 1$ are the unburned and burned faces of the flame brush respectively [17].

The turbulent consumption speed has been extensively studied for gaseous fuels [13,15,17–21]. For example, work by Venkateswaran et al. [15] investigated H₂/CO fuel blends and methane at atmospheric conditions and found a strong sensitivity of the turbulent flame speed measurements to fuel composition. This sensitivity was primarily attributed to preferential diffusion effects. Moreover, this study indicated a significant difference in turbulent flame speed for 90% H₂ fuel blends relative to other fuels with similar laminar flame speeds. This indicates that classic correlations between laminar flame speed and turbulence intensity can be insufficient for determining the turbulent flame speed. Further work by Lieuwen and colleagues in [18] on the turbulent flame speeds of H₂/CO fuel blends at pressures of 1 atm – 20 atm confirmed that different fuels with equivalent laminar flame speeds had different turbulent flame speeds.

Limited data has been reported for the turbulent flame speeds of large hydrocarbon fuels (i.e., liquid at room temperature). Goh et al. [22] reported turbulent consumption speeds for JP-10/air mixtures at 473 K and atmospheric pressure for a range of $\phi = 0.2$ to 0.8. Their results reported turbulent flame velocities with respect to experimentally determined axial root mean square (rms) velocity fluctuations and Damköhler number. These results suggest a strong sensitivity of the turbulent flame speed to turbulent time and length scales. However, these results are limited and further investigation is needed to confirm the observed trends. Won et al. [12] measured the turbulent burning velocities of n-heptane air mixtures using a Reactor Assisted Turbulent Slot (RATS) burner. The study demonstrated a strong sensitivity of the turbulent flame speed to low temperature chemistry by varying the preheat temperature while holding flow velocity constant. The study observed that pre-flame oxidation altered fuel chemistry and transport properties resulting in an increase in the turbulent flame speed. Their work concluded a strong sensitivity of the turbulent flame speed to fuel chemistry can occur.

The objective of this effort is to measure the global consumption speed of large hydrocarbon liquid fuels. This is motivated by the significance of the turbulent flame speeds in evaluating combustion performance in practical devices, and the importance of large hydrocarbon fuels. Sensitivities to fuel chemistry, bulk Reynolds number, and turbulence intensity are evaluated.

1.1 Experimental approach and facility

A schematic of the vaporizer and burner system used for generating the flames is presented in Figure 1. The burner replicates the design developed by Lieuwen and colleagues [15]. The burner allows the Reynolds number, turbulence intensity, and temperature of the flow to be independently controlled. The burner consists of a smooth contoured nozzle tapering down from 76 mm to the 12 mm exit diameter. It is designed to reduce boundary layer growth in the nozzle and achieve a top hat velocity profile at the exit [15]. An annular sinter plate, with a 20 micron nominal pore size, is positioned around the burner outlet and anchors a premixed methane-air pilot flame. The methane pilot flame operates at an equivalence ratio equal to 1; the total mass flow does not exceed 9% of the main mass flow rate. A sensitivity analysis was performed by varying the pilot flame mass flow for a range of main flame flow conditions. This analysis revealed that the pilot flame had less than a 5% impact on the turbulent flame speed for the measured conditions. The primary fuel-air mixture passes through a layer of ball bearings upon entering the burner to prevent “jetting” from the smaller diameter feed-lines and encourage uniform flow development [15]. The flow then passes through a short development length to ensure it is well mixed and has a uniform temperature and velocity distribution. A type-K thermocouple is used to monitor the final unburned temperature of the reactant flow (200 °C ~ 473 K) in this development length and has a total uncertainty of 2% of the set point temperature.

The vaporizer premixes and vaporizes the large hydrocarbon fuels. The mixing occurs ~1.3 m upstream of the burner outlet which ensures a well-mixed reactant flow. The vaporizer design replicates a system developed by Air Force Research Laboratory. Pre-heated air and room temperature fuel are injected in a solid-cone spray using an air assisted atomizing nozzle. Additional preheated air is injected into the vaporizer through an annular manifold positioned around

the fuel nozzle. The manifold creates a high velocity, heated air-curtain around the fuel injection site, encouraging turbulent mixing and preventing any fuel from contacting the heated vaporizer walls. The main air flow is systematically heated to the desired set point temperature of 200 °C (~ 473 K) using a series of tube heaters with PID temperature controllers prior to injection into the vaporizer. After mixing and vaporization the reactant fuel-air mixture is maintained at a constant 200 °C (~ 473 K) with an uncertainty of 2% of the set point value. Care is taken to keep the air temperature below auto-ignition temperatures at all times for safety and to minimize any fuel cracking that may occur.

The air flow rates for both the pilot and main flames are metered upstream of the vaporizer and preheaters using high accuracy rotameters with 3% and 2% full scale accuracy respectively. Pressure transducers with 2% full scale accuracy and type-K thermocouples with 2% full scale accuracy are used to correct for density changes caused by the preheat process along the flow path. The mass flow rate of the methane pilot fuel is metered directly using a thermal mass (MKS) flow controller with a full scale accuracy of 1%. The main fuel flowrate is metered volumetrically using dual syringe-pumps with an accuracy of 0.5% of the set point value. As a result the uncertainty of the equivalence ratios for the pilot and main flows are below 2% and 3%, respectively. The total mass flow uncertainty of the pilot methane-air mixture is below 3%.

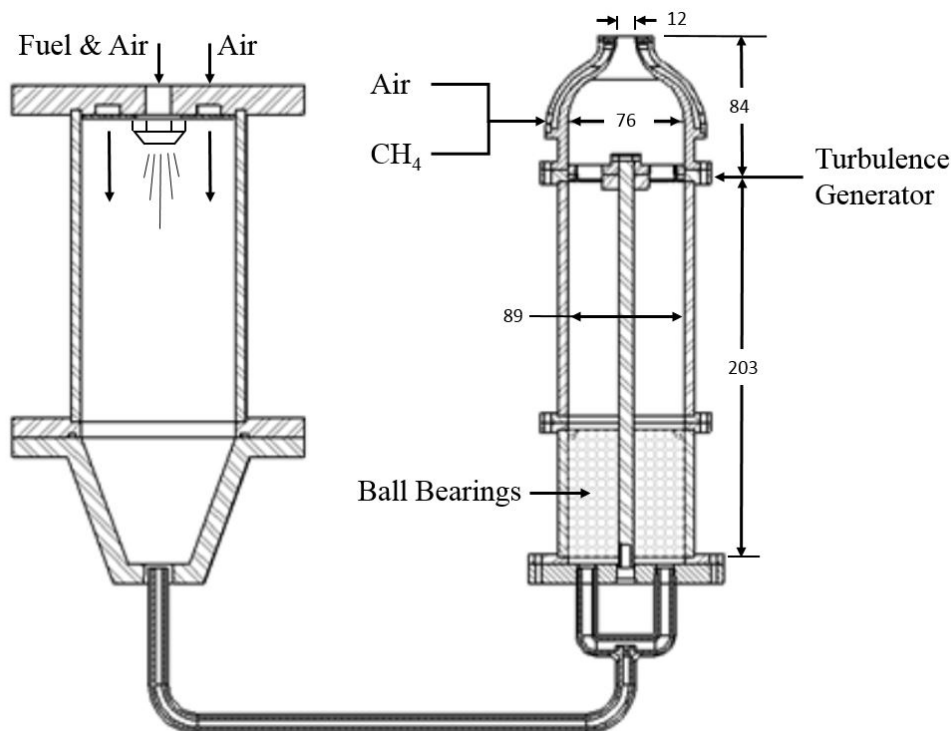


Figure 1: Schematic of the vaporizer and burner system. All dimensions in mm.

The turbulence intensity is controlled independently of the bulk fluid velocity using a turbulence generator developed by Lieuwen and colleagues [15,18]. As shown in Figure 1 the turbulence generator is located 84 mm upstream of the burner outlet and consists of a 3 mm thick bottom plate that is bolted to the plenum and a 6 mm thick top plate attached to a central shaft that extends out the bottom of the plenum. Flow straighteners are fixed to both the top and bottom plates and extend into the annular openings in the adjacent plate as shown in Figure 2. This geometry minimizes swirl that may develop in the flow at very high blockage ratios. The turbulence intensity at the exit of the burner is proportional the plate's annular position (i.e., blockage ratio). A high contrast top down photo of the plate's position is taken to determine the blockage ratio. The image is then binarized and the ratio determined. The turbulence intensities are estimated based on the blockage ratio and data reported Venkateswaran et al. [15,18] for the same burner geometry. Future work will verify the turbulence intensities using a hotwire wire anemometer probe.

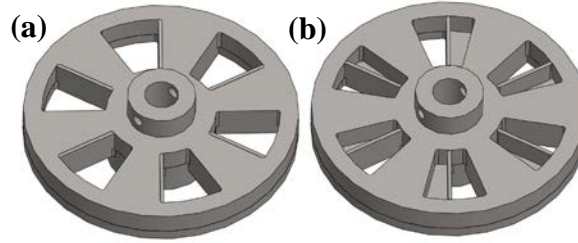


Figure 2: Schematic of turbulence generator, (a) Fully Open, (b) Partially Closed.

The turbulent consumption speeds were collected for three large hydrocarbon fuels for a range of operating conditions. Reynolds number conditions were varied from 5,000 to 10,000 for turbulence intensities of $\sim 0.13\%$ and $\sim 0.19\%$ of the bulk flow velocity. All tests were repeated for a range of equivalence ratios from 0.8-1 at atmospheric conditions with a constant preheat temperature of $T_u = 200^\circ\text{C}$ ($\sim 473\text{ K}$).

1.2 Image Processing

The $S_{T,GC}$ is determined from the reactant mass flow, density, and the mean flame brush area defined by contour $\langle c \rangle$, as shown in equation 1. The mass flow rate is measured experimentally and the density is determined from the air-fuel mass ratio metered at standard atmospheric conditions. The mean flame brush area is determined from chemiluminescence measurements using a 16-bit intensified charge-coupled device (ICCD) camera with a 1024×1024 pixel resolution and a 25 mm, f/4.0, UV camera lens. The camera system is sensitive in the visible and ultraviolet spectrum between 230-1,100 nm, and as such, is capable of measuring OH^* and CO_2^* chemiluminescence. Line-of-sight reference images are obtained over 3 minutes at a sampling rate or 1.9902 Hz to minimize bias from the pilot flame for background noise; the exposure time and gate width for these images are 0.1 s and 0.07 s, respectively.

Image processing to determine the average flame sheet from the measurements was completed using the technique developed by Venkateswaran et al. in [15] and is summarized here. Figure 3 provides an illustration of the process. The line-of-sight images are average, the time-averaged the background is subtracted, and the image is cropped, as shown in Figure 3(a). The image is then checked for axis-symmetry, straightened, and filtered using a 2-D median filter with a kernel less than 2% of the burner diameter, as seen in Figures 3(b) and 3(c). A 3 point Abel deconvolution is applied and the resulting axial distribution of the centerline intensity is fit to a Gaussian curve. The maximum intensity location is determined. This allows the leading edge of the time averaged flame-brush to be determined. This point is the most probable location of the flame brush, and is defined as the $\langle c \rangle = 0.5$ progress variable contour and corresponds to the location of maximum intensity [15], as shown in Figure 3(d). The estimated uncertainty in this process is 1%-2% [15].

Two lines are then drawn from the determined location of the maximum intensity to the flame anchor points and rotated to generate a cone. Figure 3(d) shows the $\langle c \rangle = 0.5$ surface drawn on the flame. The outer surface area of the resulting cone is used as $\bar{A}_{\langle c \rangle}$ in the $S_{T,GC}$ calculation. The overall uncertainty in the $S_{T,GC}$ calculation is estimated to be below 4%, based instrumentation uncertainty propagation determined using a Kline McClintock uncertainty analysis. All error bars presented represent both this instrumentation biased as well as precision uncertainty from all repeatability data.

1.3 Fuel Analysis

Three fuels were considered in this study, namely a conventional Jet-A blend, as well as two experimental blends referred to as C1 and C5. These fuels have been selected to investigate potential sensitivities to fuel chemistry observed in the literature. Jet-A is a primary reference due to the large amount of available literature to validate against, and is compared to a bimodal blend of iso-dodecane and iso-hexadecane (C1), and a mix of iso-decane, n-decane, and C3-benzene

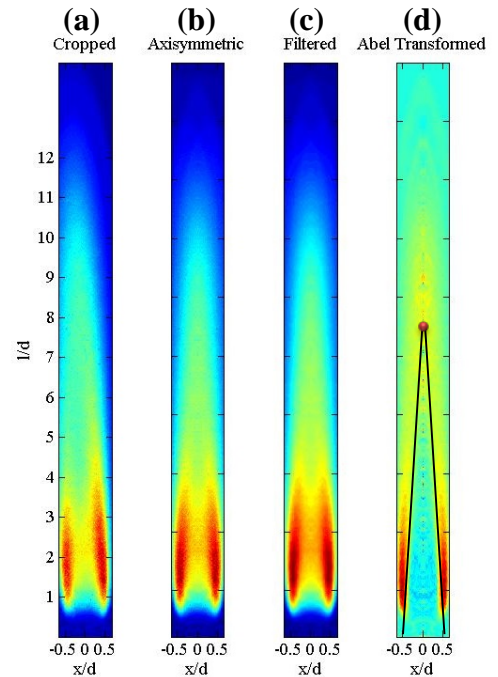


Figure 3: Step-by-step summary of image processing approach: (a) time-averaged, background subtracted and cropped (b) Axisymmetric (c) 2-D median filtered (d) Abel transform with $\langle c \rangle = 0.5$ contour drawn.

(C5). These surrogates have been selected to investigate suggested sensitivities to aromatic and alkane content as well as species carbon number. Each of the fuels have similar lower heating values and densities as indicated in Table 1. However, these fuels have dramatically different fuel compositions, as indicated by the average molecular formulas and molecular weights.

Table 1: Average fuel properties for selected fuel blends.

Fuel	Average Molecular Formula	Molecular Weight [g/mol]	LHV [MJ/kg]	ρ [kg/m ³]
Jet-A	C _{11.4} H _{22.1}	158.6	43.0	804
C1	C _{12.9} H _{26.8}	181.9	43.6	782
C5	C _{9.7} H _{18.7}	135.4	42.8	770

The differences in the chemical classes within the fuels are further highlighted in Appendix A, Figures 7-9. These bar graphs indicate the distribution of components within the aromatic, alkane, cycloalkane, and alkene groups of the fuels relative to species carbon number. Notice that Jet-A has a near Gaussian distribution of equal parts aromatic, alkane, and cycloalkanes relative to carbon number. Whereas C1 is predominantly branched alkanes, and C5 is a mix of branched and straight alkanes, and aromatics. Note that these fuels isolate both species chemical class as well as species carbon number. C1 in particular is a bimodal blend of C-12 and C-16 alkanes while C5 is comprised of species with C-10 carbon numbers and below. As a result, these fuels highlight fuel chemistry sensitivities to alkane and aromatic content as well differences in species carbon content, while maintaining similar lower heating values.









2 Results and Discussion

The turbulent consumption speeds for the three fuels at $Re_D = 10,000$ and two estimated turbulence intensities are presented relative to the fuel-to-air ratio and equivalence ratio in the left and right panels of Figure 4 (respectively). The equivalence ratio is based on stoichiometry found using the average molecular formula whereas the air-to-fuel mass ratio is explicitly controlled. Error bars represent the total bias and precision uncertainty within 95% confidence. Table 2 provides a summary of the marker convention used in presenting the different flame conditions. The data shows a sensitivity to fuel composition at both turbulence conditions. The Jet-A flame (circles) has a consistently higher flame speed relative to the other fuels. For example, the turbulent flame speed is 6% higher than C1 (triangles) and 11% higher than C5 (squares) at stoichiometric conditions for the low turbulence intensity. In addition, there is a 14% increase in the turbulent flame speed of Jet-A from the minimum (0.85) to maximum (1) equivalence ratio conditions for both turbulence intensities. In contrast there is only a 6% to 7% increase in the turbulent flames speeds of C1 and C5 flames respectively under similar conditions. Note that there is less than a 1% and 3% difference in the turbulent flame speed between Jet-A and C1 and C5 (respectively) near the lean stability limits. All of the fuels respond similarly to increases in turbulence intensity, despite differences in fuel chemistry. The turbulent flame speeds of all three fuels increases an average of 35% across all equivalence ratios between the ~13% (closed symbols) and ~19% (open symbols) turbulence intensity cases. Notice that irrespective of the turbulence intensities, the turbulent flame speeds have similar values near the lean blow off limits.

Similar trends in turbulent flame speeds have been observed in laminar flames. As discussed previously, Kumar et al. [3] measured laminar flame speeds for Jet-A, S-8, and n-decane using twin counter flow burners. For Jet-A flames, at similar temperature and pressure conditions, with $\phi \sim 0.85$ and $\phi \sim 1$ they observed laminar flame speeds of $S_L \sim 0.75$ m/s and $S_L \sim 0.85$ m/s respectively; this result suggests a 65% nominal increase between laminar and turbulent flame conditions. Note also that, similar to the turbulent flame trend, there is ~14% increase in the laminar flame speed between the stated equivalence values ranges. Moreover, when comparing Jet-A to the other alternative fuels studied, results observed by Kumar et al. show a similar converging trend for the laminar flame speed at the lean extinction limit. This similarity between laminar and turbulent flame trends suggests that these trends are the result of fuel chemistry effects rather than flow conditions.

The flame speed and their corresponding adiabatic flame temperatures are reported in Figure 5 to allow investigation of the effect of the flame temperature on the turbulent flame speed. Note that there are no notable differences in the observed trends. This shows that the turbulent flame speed is largely insensitive to the adiabatic flame temperature for these fuels.

Table 2: Table legend for turbulent consumption speed data.

Re_D	Jet-A		C1		C5	
	$\frac{u'_{rms}}{U} \sim 0.13$	$\frac{u'_{rms}}{U} \sim 0.19$	$\frac{u'_{rms}}{U} \sim 0.13$	$\frac{u'_{rms}}{U} \sim 0.19$	$\frac{u'_{rms}}{U} \sim 0.13$	$\frac{u'_{rms}}{U} \sim 0.19$
5,000						
7,500						
10,000						

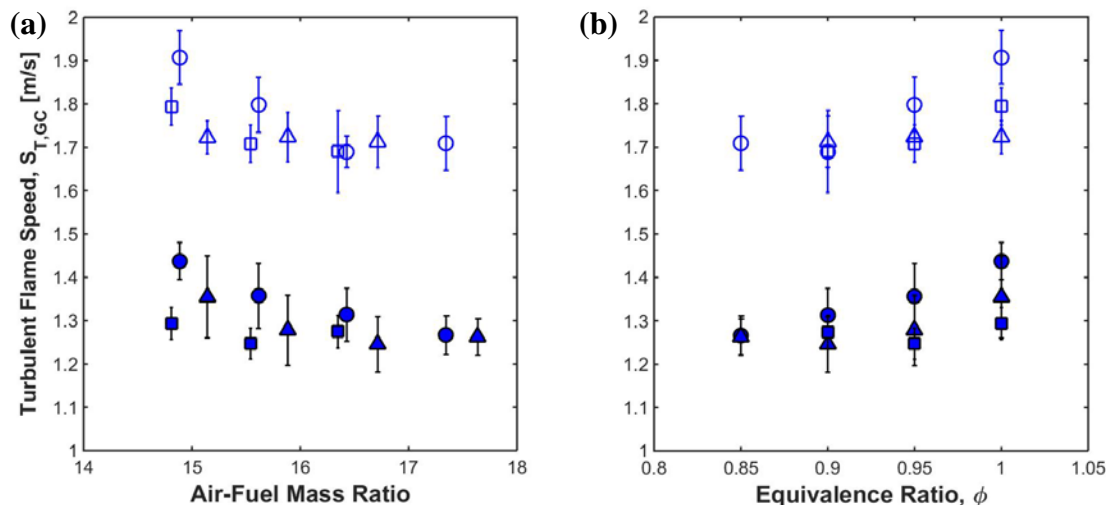


Figure 4: Turbulent flame speed of Jet-A/Air mixture compared to alternative fuel blends C1 and C5 relative to (a) air-fuel mass ratio and (b) equivalence ratio at a Reynolds number of 10,000 and two turbulence intensities.

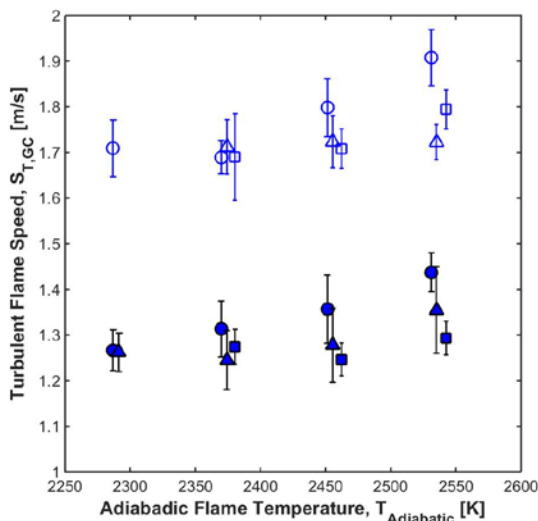


Figure 5: Turbulent flame speed of Jet-A/Air mixture compared to alternative fuel blends C1 and C5 relative to adiabatic flame temperature at a Reynolds number of 10,000 and two turbulence intensities.

The equivalence ratio of the three fuels at lean blow-off are different, despite similarities in the turbulent flame speeds. Jet-A was the only fuel stable for the maximum turbulence intensity at $\phi = 0.85$. The other fuels tend to form visibly broken reaction fronts at these lean conditions with high turbulence intensities making turbulent flame measurements infeasible; thus, turbulent flame speeds are not presented for these conditions. Continued reduction of the equivalence ratio beyond this broken reaction regime results in blow-off. Reducing the turbulence intensity results in visibly increased stability for all three fuels. C1 forms a visibly closed reaction front at an equivalence ratio of 0.85 for the low turbulence intensity and as a result has a measureable turbulent flame speed. In contrast the C5 reaction front remains broken at this equivalence ratio despite reduction in the turbulence intensity. The sensitivity to lean blow-off for C1 and C5, in comparison to Jet-A, is attributed to reduced reaction rates, reducing the mass burning fluxes.

The sensitivity of the turbulent consumption speed and flame stability to fuel chemistry is attributed to differences in the reaction rates of the primary fuel constituents. The higher flame speed of the conventional Jet-A blend corresponds to the higher percentage (by weight) of straight chain alkanes relative to the branched alkanes and aromatics dominant in the other fuels. Typically straight chain alkanes of equivalent carbon number have faster reactions rates than branched alkanes or aromatics, and branched alkanes are typically more reactive than aromatics [4,6,23,24]. Similarly, hydrocarbon species with a higher carbon number will oxidize more readily than lower carbon number species as longer chains are less stable and break down more readily into radicals during the oxidation process [1]. It follows that C1 should have an increased

flame speed relative to C5 as it has an average of 13 carbon atoms per chain and is nearly 100% branched alkanes whereas C5 has an average carbon number of 10 and a large aromatic component (~30%). Thus, C5 should have a slower flame speed because of reduced reaction rates associated with high aromatic content. This trend is observed in the data except at an equivalence ratio of unity at the maximum turbulence intensity.

Figure 6 presents the turbulent flame speed of Jet-A for $5,000 < Re_D < 10,000$ for a range of air-to-fuel ratios (left panel) and equivalence ratios (right panel). All four of the Reynolds number and turbulence intensity conditions presented exhibit similar trends for the different equivalence ratios and air-to-fuel ratios. There is a 40% average increase in turbulent flame speed between the $Re_D = 5,000$ and the $Re_D = 10,000$ cases. This result shows a sensitivity of the turbulent flame speed to the Reynolds number. As the Reynolds number increases the turbulence intensity also increases. Increases in turbulence intensity increase the turbulent flame speed by further wrinkling of the flame front. The trends observed here for large hydrocarbon fuels agree with those reported for gaseous fuels [18], which showed that increases in Reynolds number increase the turbulent flame speed. This increase was attributed to an increase in the absolute magnitude of turbulent fluctuations inherent to higher Reynolds number flows.

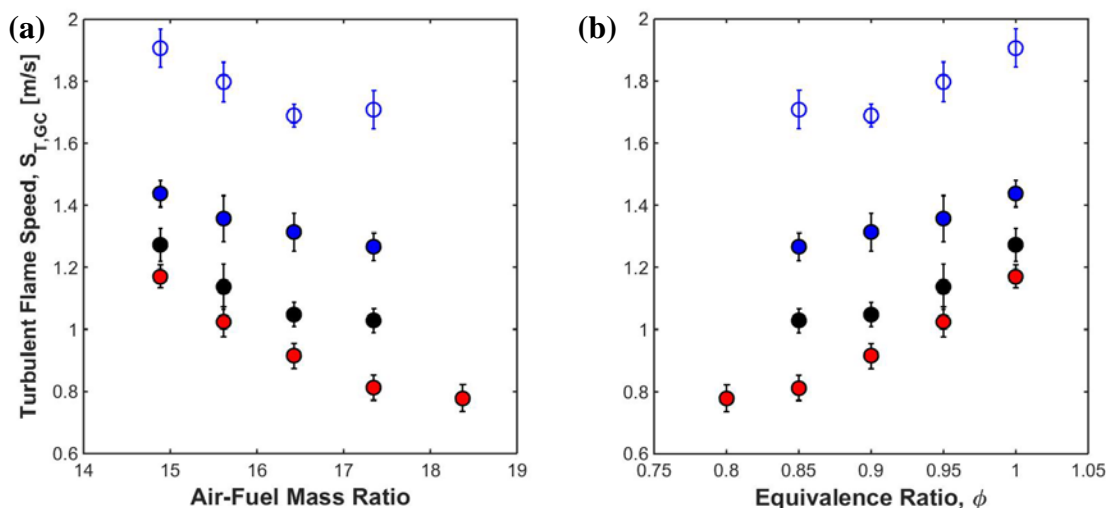


Figure 6: Turbulent flame speed of Jet-A/Air mixture plotted against (a) air-fuel mass ratio and (b) equivalence ratio for various Reynolds numbers and turbulence intensities.

An increase in flame stability is noted for decreasing Reynolds number. Additional flame speeds were collected at the equivalence ratio equal to 0.8 for the $Re_D = 5,000$ flame. Thus the flame is able to remain stable at leaner conditions. The data also shows an increased sensitivity of the turbulent flame speed to Reynolds number at decreased equivalence ratios. Notice, the percent increase in turbulent flames speeds between Reynolds number cases is greatest at low equivalence ratios. At an $\phi = 0.85$ the increase in flame speed between the $Re_D = 5,000$ and $Re_D = 7,500$ cases is 27% with a 23% increase observed between the $Re_D = 7,500$ and $Re_D = 10,000$ cases. These differences are significant when compared to stoichiometric conditions which have 9% and 13% increases respectively for the same increases in Reynolds number. This trend could suggest a sensitivity to flame stretch. Similar results have been observed for laminar flames in [3].

3 Summary

Turbulent consumption speeds for large hydrocarbon fuels are reported in this work. A fuel sensitivity of the turbulent flame speed is observed, despite the similar heat release rates. Moreover, this fuel sensitivity is evident from differences in the lean blow-off limits of the three fuels. Jet-A had the highest turbulent flame speeds and largest stability range while C5 has the slowest turbulent flame speeds and smallest stability range. This sensitivity corresponds to the aromatic and alkane content within the fuels, with slower flame speeds and decreased stability ranges corresponding to fuels with higher concentrations of less reactive fuel constituents. The turbulent flame speed was found to increase with increased turbulence intensity for all three fuels suggesting a sensitivity of the turbulent flame speed to turbulent chemistry interactions. This trend is attributed to increased wrinkling of the flame brush resulting from increases in the absolute magnitude of turbulent fluctuations. A similar sensitivity of the turbulent flame speed to Reynolds number was also observed for Jet-A. A potential sensitivity of the turbulent flame speed to flame stretch was observed in Jet-A. However, further investigation is needed to confirm this conclusion.

4 Acknowledgements

This work was funded by the US Federal Aviation Administration (FAA) Office of Environment and Energy as a part of ASCENT Project 27B under FAA Award Number: 13-C-AJFE-OSU-02. Any opinions, findings, and conclusions or recommendations expressed in this material are those of the authors and do not necessarily reflect the views of the FAA or other ASCENT Sponsors. The authors would like to thank Dr. Tim Lieuwen and colleagues for the burner specifications and assistance in assembly the experimental facilities, Dr. Scott Stouffer (University of Dayton Research Institute) and the Air Force Research Laboratory (AFRL) for the vaporizer design, Dr. Tim Edwards from AFRL for supplying the fuel samples of Jet-A, C1, and C5, and Mick Carter and Johnathan Bonebrake for assistance with data collection.

5 References

- [1] C.K. Law, Combustion Physics, 1st ed., Cambridge University Press, New York, 2006.
- [2] X. Hui, C.-J. Sung, Fuel 109 (2013) 191–200.
- [3] K. Kumar, C.-J. Sung, X. Hui, Fuel 90 (2011) 1004–1011.
- [4] K. Kumar, J.E. Freeh, C.J. Sung, Y. Huang, J. Propuls. Power 23 (2007) 428–436.
- [5] C. Dong, Q. Zhou, Q. Zhao, Y. Zhang, T. Xu, S. Hui, Fuel 88 (2009) 1858–1863.
- [6] S.G. Davis, C.K. Law, Symp. Combust. 27 (1998) 521–527.
- [7] A.E. Bakali, J.-L. Delfau, C. Vovelle, Combust. Sci. Technol. 140 (1998) 69–91.
- [8] J.M. Simmie, Prog. Energy Combust. Sci. 29 (2003) 599–634.
- [9] R. Seiser, H. Pitsch, K. Seshadri, W.J. Pitz, H.J. Curran, Proc. Combust. Inst. 28 (2000) 2029–2037.
- [10] T.J. Held, A.J. Marchese, F.L. Dryer, Combust. Sci. Technol. 123 (1997) 107–146.
- [11] H.J. Curran, P. Gaffuri, W.J. Pitz, C.K. Westbrook, Combust. Flame 129 (2002) 253–280.
- [12] S.H. Won, B. Windom, B. Jiang, Y. Ju, Combust. Flame 161 (2014) 475–483.
- [13] R.K. Gouldin, F., and Cheng, Int. Work. Premixed Turbulent Flames (2010).
- [14] R.K. Cheng, in: T.C. Lieuwen, Y. V., R.A. Yetter (Eds.), Synth. Gas Combust. Fundam. Appl., Boca Raton, FL, 2009, p. 403.
- [15] P. Venkateswaran, A. Marshall, D.H. Shin, D. Noble, J. Seitzman, T. Lieuwen, Combust. Flame 158 (2011) 1602–1614.
- [16] J. DRISCOLL, Prog. Energy Combust. Sci. 34 (2008) 91–134.
- [17] H. Kobayashi, T. Tamura, K. Maruta, T. Niioka, F. a. Williams, Symp. Combust. 26 (1996) 389–396.
- [18] P. Venkateswaran, A. Marshal, J. Seitzman, T. Lieuwen, J. Eng. Gas Turbines Power 136 (2013) 011504.
- [19] H. Kobayashi, K. Seyama, H. Hagiwara, Y. Ogami, R. Aldredge, Proc. Combust. Inst. 30 I (2005) 827–834.
- [20] H. Kobayashi, Y. Kawabata, K. Maruta, Symp. Combust. 27 (1998) 941–948.
- [21] H. Kobayashi, Exp. Therm. Fluid Sci. 26 (2002) 375–387.
- [22] K.H.H. Goh, P. Geipel, F. Hampf, R.P. Lindstedt, Proc. Combust. Inst. (2012).
- [23] D. SG, W. H, B. K, L. CK, Proc Combust Inst 26 (1996) 1025–1033.
- [24] Y. Huang, C.J. Sung, J. a. Eng, Combust. Flame 139 (2004) 239–251.

6 Appendix A

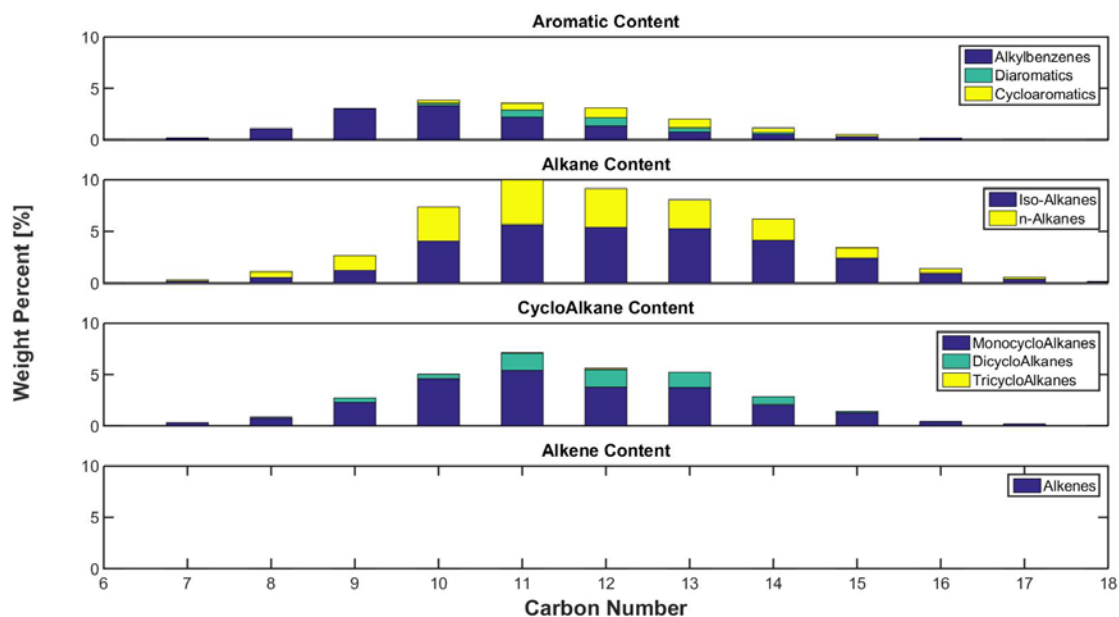


Figure 7: Fuel species composition by weight percent, presented relative to carbon number for Jet-A.

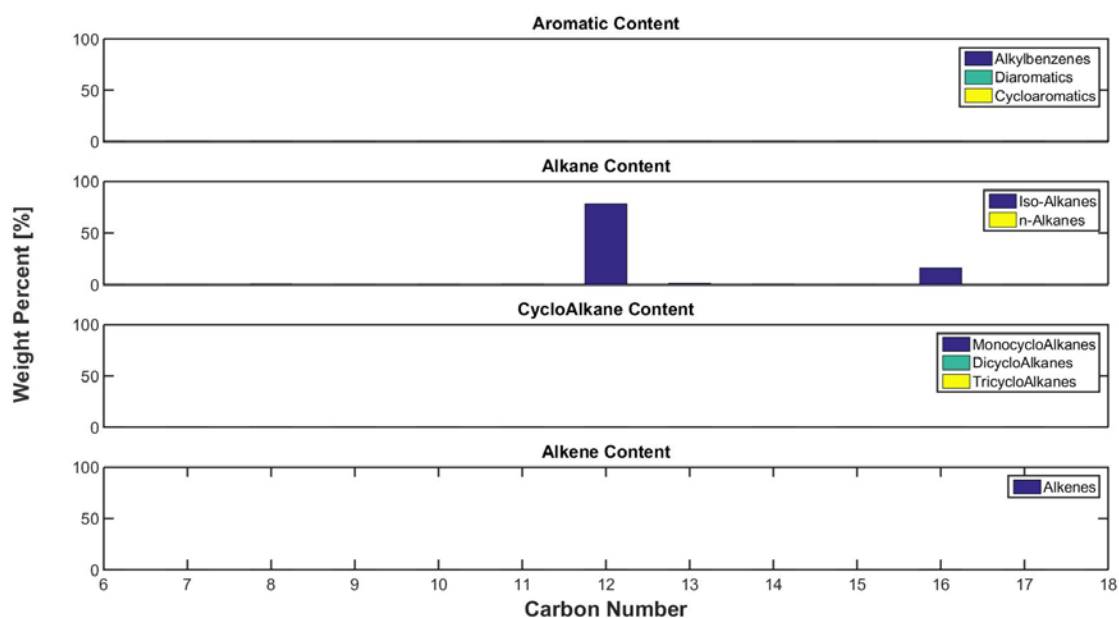


Figure 8: Fuel species composition by weight percent, presented relative to carbon number for C1 surrogate.

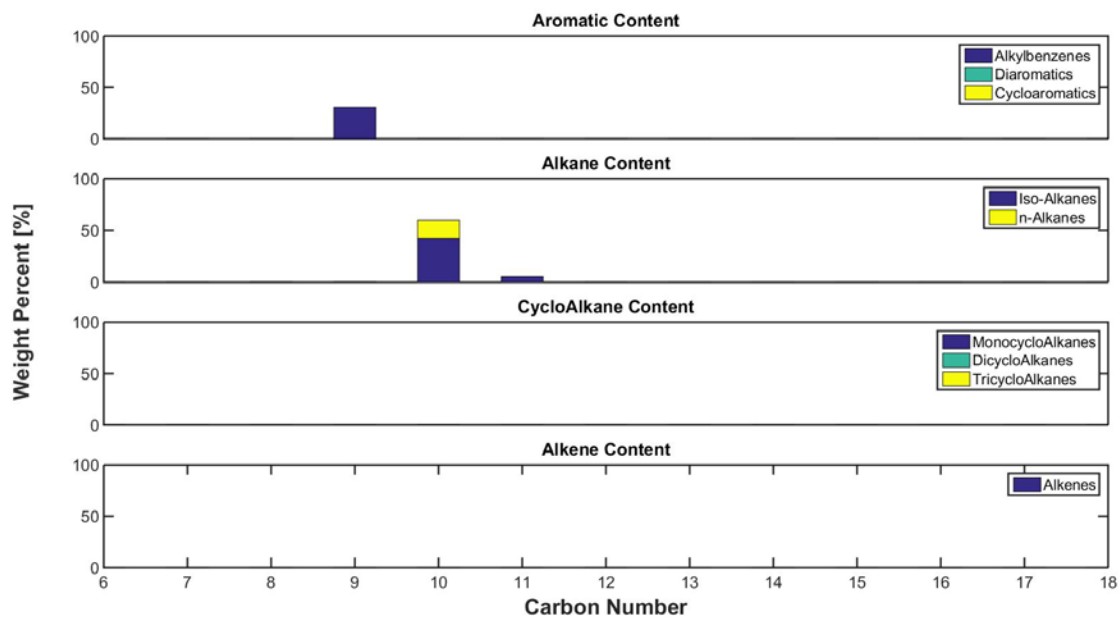


Figure 9: Fuel species composition by weight percent, presented relative to carbon number for C5 surrogate.